Available online at www.sciencedirect.com
ScienceDirect
Journal of Sound and Vibration 314 (2008) 228–245
JOURNAL OF SOUND AND VIBRATION
www.elsevier.com/locate/jsvi

Symmetry and bifurcations of a two-degree-of-freedom vibro-impact system

Y. Yue*, J.H. Xie

Department of Applied Mechanics and Engineering, Southwest Jiaotong University, Chengdu 610031, China

Received 22 August 2007; received in revised form 22 August 2007; accepted 4 January 2008
Handling Editor: L.G. Tham
Available online 14 February 2008

Abstract

A two-degree-of-freedom system with impact is considered. The symmetry of the system and its Poincaré map is described. The symmetric period $n-2$ motion corresponding to the symmetric fixed point of the Poincaré map is obtained. If the Jacobian matrix of the Poincaré map at the fixed point has a real eigenvalue crossing the unit circle at $+1$, the symmetric fixed point will bifurcate into two antisymmetric fixed points, which have the same stability via pitchfork bifurcation. The numerical simulation shows that the symmetric fixed points may have pitchfork bifurcations and Hopf bifurcations. While the control parameter changes continuously, the two antisymmetric fixed points will give birth to two synchronous bifurcation sequences.

1. Introduction

It makes extensively practical sense to research into the vibro-impact system having small clearances between the moving components. The clearances exist inevitably between the parts of the machinery due to various factors. The moving parts will collide with each other while the amplitude goes beyond the critical value. Because of the existence of impacts, the dynamics of the system is discontinuous and strongly nonlinear. On the one hand, impacts between the components take great disadvantage to the system, so the collision should be tried to avoid when the optimization design of machinery with gaps is considered. On the other hand, impacts between the components are often used to reach some special purpose.

The period-doubling bifurcation cascade in a vibro-impact system was observed numerically by Shaw and Holmes [1]. Nonlinear dynamics and the bifurcation behavior associated with impact oscillators have been studied in Refs. [2,3]. Virgin and Begley [4] described some interesting global dynamic behavior of an impact oscillator with Coulomb damping. An algorithm was applied for the calculation of the Lyapunov exponents for mechanical systems with impacts in Ref. [5]. Hopf bifurcations of symmetrical and antisymmetrical motions are shown to exist in a two-degree-of-freedom vibratory system with impact in Ref. [6]. Dynamics of a vibro-impact system is studied with special attention to interaction of Hopf and period-doubling bifurcations

*Corresponding author. Tel.: +86 28 87668987; fax: +86 28 87600797.
E-mail addresses: peak8668@yahoo.com.cn (Y. Yue), jhxie2000@126.com (J.H. Xie).

0022-460X/$ - see front matter © 2008 Elsevier Ltd. All rights reserved.
doi:10.1016/j.jsv.2008.01.003

[7]. Xie and Ding [8] considered the Hopf–Hopf bifurcation of a three-degree-of-freedom vibro-impact system, and proved that there exists the torus $\mathbf{T}^1$ and $\mathbf{T}^2$ bifurcation. Wagg [9] investigated the rising phenomena, which occurs in sticking solutions in a two-degree-of-freedom impact system. Ben-Tal [10] shows that solutions for a class of symmetric forced oscillators can be symmetric or non-symmetric, and solutions lose or gain the symmetry at a bifurcation point as a physical parameter is varied. The periodic impact motions of passengers in a vehicle traveling on rough terrain were investigated through a linear model of vehicle and passenger systems in Ref. [11]. Luo and Chen [12] presented a piecewise linear system to model the vibration of gear transmission systems, and studied the periodic motions of the system.

We show that the symmetry of the system has great influence on the dynamics of the system. As a general rule, the symmetric fixed point undergoes firstly a pitchfork bifurcation and gives birth to two antisymmetric fixed points, which have the same stability. As the parameter of the system changes continuously, the two antisymmetric fixed points will produce two synchronous bifurcation sequences, respectively.

2. Mechanical model

A two-degree-of-freedom system subjected to periodic excitation is shown in Fig. 1. The system has two masses M_1 and M_2. M_1 and M_2 are connected to two rigid planes via two linear springs K_1 and K_2, and two dampers C_1 and C_2, respectively. The excitations on both masses are harmonic with amplitudes P_1 and P_2. The excitation frequency Ω and phase angle τ are the same for the both excitations. For the small amplitudes of the excitations, the system undergoes simple oscillation and behaves as a linear system. However, as the amplitudes increased, M_2 begins to collide with stops on M_1, and the system then becomes discontinuous and nonlinear. The impact is described by coefficient of restitution R. It is assumed that the duration of impact is negligible compared with the period of the force, and the friction between M_1 and M_2 is negligible, too.

When M_2 collides with M_1 at the right and the left stop, the coordinates of M_1 and M_2 satisfy the following relationships:

$$X_2 - X_1 = \pm B. \tag{1}$$

Between any two consecutive impacts, we have

$$|X_2 - X_1| < B \tag{2}$$

and the non-dimensional differential equations of motion are given by

$$\begin{aligned} &\ddot{x}_1 + 2\zeta\dot{x}_1 + x_1 = (1 - f_2)\sin(\omega t + \tau), \\ &u_m\ddot{x}_2 + 2u_c\zeta\dot{x}_2 + u_k x_2 = f_2 \sin(\omega t + \tau), \end{aligned} \tag{3}$$

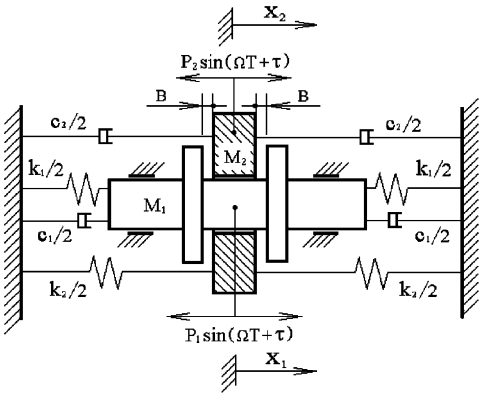

Fig. 1. Symmetric vibro-impact system.

where the non-dimensional variables and parameters are

$$u_m = \frac{M_2}{M_1}, \quad u_k = \frac{K_2}{K_1}, \quad u_C = \frac{C_2}{C_1}, \quad f_2 = \frac{P_2}{P_1 + P_2},$$
$$\omega = \Omega\sqrt{\frac{M_1}{K_1}}, \quad \zeta = \frac{C_1}{2\sqrt{K_1 M_1}}, \quad t = T\sqrt{\frac{K_1}{M_1}}, \quad x_i = \frac{X_i K_1}{P_1 + P_2}, \quad i = 1, 2. \tag{4}$$

The velocities of the two masses after impacting can be obtained:

$$\dot{x}_{1+} = a\dot{x}_{1-} + b\dot{x}_{2-},$$
$$\dot{x}_{2+} = c\dot{x}_{1-} + d\dot{x}_{2-}, \tag{5}$$

where

$$a = \frac{1 - u_m R}{1 + u_m}, \quad b = \frac{u_m(1 + R)}{1 + u_m}, \quad c = \frac{1 + R}{1 + u_m}, \quad d = \frac{u_m - R}{1 + u_m}. \tag{6}$$

In Eq. (5), dot $(\cdot)$ denotes differentiation with the non-dimensional time t. $\dot{x}_{i-}$ and $\dot{x}_{i+}$ $(i = 1,2)$ represent the non-dimensional velocities of M_i before and after impact, respectively. When M_2 collides with the right stop of M_1, the non-dimensional displacements of two masses satisfy

$$x_2 - x_1 = b_f \tag{7}$$

and when M_2 collides with the left stop of M_1, we have

$$x_2 - x_1 = -b_f, \tag{8}$$

where

$$b_f = \frac{K_1 B}{P_1 + P_2}. \tag{9}$$

The general solution of Eq. (3) is given by

$$x_1 = \mathrm{e}^{-\zeta t}(A_1 \cos(\omega_{d1} t) + A_2 \sin(\omega_{d1} t)) + B_1 \sin(\omega t + \tau) + B_2 \cos(\omega t + \tau),$$
$$x_2 = \mathrm{e}^{-\eta t}(A_3 \cos(\omega_{d2} t) + A_4 \sin(\omega_{d2} t)) + B_3 \sin(\omega t + \tau) + B_4 \cos(\omega t + \tau), \tag{10}$$

where

$$\eta = \frac{u_c \zeta}{u_m}, \quad u = \frac{u_k}{u_m}, \quad \omega_{d1} = \sqrt{1 - \zeta^2}, \quad \omega_{d2} = \sqrt{u - \eta^2} \tag{11}$$

and A_i $(i = 1, 2, 3, 4)$ are the integration constants determined by the initial conditions, B_i are the amplitude constants given by

$$B_1 = \frac{(1 - \omega^2)(1 - f_2)}{(1 - \omega^2)^2 + 4\zeta^2\omega^2}, \quad B_2 = -\frac{2\zeta\omega(1 - f_2)}{(1 - \omega^2)^2 + 4\zeta^2\omega^2},$$
$$B_3 = \frac{(u_k - u_m\omega^2) f_2}{(u_k - u_m\omega^2)^2 + 4u_c^2\zeta^2\omega^2}, \quad B_4 = -\frac{2u_c\zeta\omega f_2}{(u_k - u_m\omega^2)^2 + 4u_c^2\zeta^2\omega^2}. \tag{12}$$

3. Symmetric period n−2 motion

Suppose that M_2 collides with the right stop of M_1 at first, and the origin of the time coordinate is displaced to this moment ($t = t_0 = 0$). Subsequently, after $n/2$ forcing period ($t = t_1 = n\pi/\omega$, and n is an odd number), M_2 collides with the left stop. At the moment $t = t_2 = 2n\pi/\omega$, M_2 collides with the right stop once again. The periodic motion will be called symmetric period n−2 motion if all the following relationships

are satisfied:

$$x_1(t_1) = -x_1(t_0), \quad \dot{x}_{1+}(t_1) = -\dot{x}_{1+}(t_0), \quad x_2(t_1) = -x_2(t_0), \quad \dot{x}_{2+}(t_1) = -\dot{x}_{2+}(t_0),$$
$$x_1(t_2) = x_1(t_0), \quad \dot{x}_{1+}(t_2) = \dot{x}_{1+}(t_0), \quad x_2(t_2) = x_2(t_0), \quad \dot{x}_{2+}(t_2) = \dot{x}_{2+}(t_0), \tag{13}$$

where $x_i(t_j)$ and $\dot{x}_{i+}(t_j)$ represent, respectively, the non-dimensional displacements and velocities of M_i $(i = 1, 2)$ after impacting at t_j $(j = 0, 1, 2)$.

Proposition 1. *If there are initial conditions* $\tau = \tau_0$, $x_1(0) = x_{10}$, $\dot{x}_{1+}(0) = y_{10}$, $x_2(0) = x_{20}$, $\dot{x}_{2+}(0) = y_{20}$ *which result in*

$$\begin{aligned}
&x_2(0) - x_1(0) = b_f, \quad x_2(t_1) - x_1(t_1) = -b_f,\\
&x_1(0) = -x_1(t_1), \quad x_2(0) = -x_2(t_1),\\
&\dot{x}_{1+}(0) = -\dot{x}_{1+}(t_1) = -[a\dot{x}_{1-}(t_1) + b\dot{x}_{2-}(t_1)],\\
&\dot{x}_{2+}(0) = -x_{2+}(t_1) = -[c\dot{x}_{1-}(t_1) + d\dot{x}_{2-}(t_1)],\\
&\left|x_1(t) - x_2(t)\right| \leqslant b_f, \quad t \in [0, t_1],
\end{aligned} \tag{14}$$

then the symmetric period $n-2$ *motion of the system exists, and can be expressed by*

$$x_i(t) = \begin{cases} x_i(t), t \in [0, t_1] \\ -x_i(t - t_1), t \in [t_1, t_2] \end{cases}, \quad i = 1, 2. \tag{15}$$

Inserting the boundary conditions (14) into solutions (10), we obtain

$$\begin{aligned}
w_1 A_1 &= l_1 \cos\tau_0 + u_1 \sin\tau_0 - v_1 b_f,\\
w_2 A_1 &= l_2 \cos\tau_0 + u_2 \sin\tau_0 - v_2 b_f,
\end{aligned} \tag{16}$$

such that the phase angle and the integration constants can be solved (see Appendix A). It should be noted that the existence of the symmetric period $n-2$ motion requires the conditions:

$$\begin{aligned}
&(u_1 w_2 - u_2 w_1)^2 + (l_1 w_2 - l_2 w_1)^2 - (w_1 v_2 - w_2 v_1)^2 b_f^2 \geqslant 0,\\
&l_1 w_2 - l_2 w_1 + (w_2 v_1 - w_1 v_2) b_f \neq 0, \quad w_1 \neq 0, \quad w_2 \neq 0,\\
&\omega \neq \frac{2n}{k}\omega_{d1}, \quad k = 1, 2, 3 \ldots,\\
&\omega \neq \frac{4n}{2k+1}\omega_{d2}, \quad k = 0, 1, 2, 3 \ldots,
\end{aligned} \tag{17}$$

where u_i, w_i, l_i, v_i, $(i = 1, 2)$ are given in Appendix A, too.

Substituting the phase angle and the integration constants into solution (10), we obtain the symmetric period $n-2$ solution:

$$x_1 = \begin{cases} e^{-\zeta t}[A_1 \cos(\omega_{d1} t) + A_2 \sin(\omega_{d1} t)] + B_1 \sin(\omega t + \tau_0) + B_2 \cos(\omega t + \tau_0), & t \in [0, t_1], \\ e^{-\zeta(t-t_1)}[A_1' \cos(\omega_{d1}(t - t_1)) + A_2' \sin(\omega_{d1}(t - t_1))] + B_1 \sin(\omega t + \tau_0') + B_2 \cos(\omega t + \tau_0'), & t \in [t_1, t_2], \end{cases} \tag{18}$$

$$x_2 = \begin{cases} e^{-\eta t}[A_3 \cos(\omega_{d2} t) + A_4 \sin(\omega_{d2} t)] + B_3 \sin(\omega t + \tau_0) + B_4 \cos(\omega t + \tau_0), & t \in [0, t_1], \\ e^{-\eta(t-t_1)}[A_3' \cos(\omega_{d2}(t - t_1)) + A_4' \sin(\omega_{d2}(t - t_1))] + B_3 \sin(\omega t + \tau_0') + B_4 \cos(\omega t + \tau_0'), & t \in [t_1, t_2], \end{cases} \tag{19}$$

where the integration constants A_i and A_i' $(i=1,2,3,4)$ are the functions of the initial conditions $(\dot{x}_{10}, x_{20}, \dot{x}_{20}, \tau_0)$ and $(\dot{x}_{10}', x_{20}', \dot{x}_{20}', \tau_0')$, respectively:

$$\begin{aligned}
A_1 &= -B_1 \sin\tau_0 - B_2\cos\tau_0 + x_{20} + b_f,\\
A_2 &= \frac{1}{\omega_{d1}}((-\zeta B + \omega B_2)\sin\tau_0 - (\zeta B_2 + \omega B_1)\cos\tau_0 + \zeta x_{20} + \zeta b_f),\\
A_3 &= -B_3 \sin\tau_0 - B_4\cos\tau_0 + x_{20},\\
A_4 &= \frac{1}{\omega_{d2}}((-\eta B_3 + \omega B_4)\sin\tau_0 - (\eta B_4 + \omega B_3)\cos\tau_0 + \eta x_{20} + \dot{x}_{20},
\end{aligned} \tag{20}$$

$$\begin{aligned}
A_1' &= -B_1 \sin\tau_0' - B_2\cos\tau_0' + x_{20}' - b_f,\\
A_2' &= \frac{1}{\omega_{d1}}\left[(-\zeta B_1 + \omega B_2)\sin\tau_0' - (\zeta B_2 + \omega B_1)\cos\tau_0'\right] + \zeta x_{20}' + \dot{x}_{10}' - \zeta b_f,\\
A_3' &= -B_3 \sin\tau_0' - B_4\cos\tau_0' + x_{20}',\\
A_4' &= \frac{1}{\omega_{d2}}\left[(-\eta B_3 + \omega B_4)\sin\tau_0' - (\eta B_4 + \omega B_3)\cos\tau_0' + \eta x_{20}' + \dot{x}_{20}'\right]
\end{aligned} \tag{21}$$

and the two sets of initial condition satisfy

$$(\dot{x}_{10}', x_{20}', \dot{x}_{20}', \tau_0') = (-\dot{x}_{10}, -x_{20}, -\dot{x}_{20}, \tau_0 + n\pi). \tag{22}$$

4. Poincaré map and its symmetry

Eq. (3) can be rewritten as

$$\begin{aligned}
\dot{x}_1 &= y_1,\\
\dot{y}_1 &= -x_1 - 2\zeta y_1 + (1-f_2)\sin(\omega t + \tau),\\
\dot{x}_2 &= y_2,\\
\dot{y}_2 &= \frac{1}{u_m}(-u_k x_2 - 2u_c\zeta y_2 + f_2\sin(\omega t + \tau)).
\end{aligned} \tag{23}$$

Equivalently,

$$\dot{\mathbf{X}} = \mathbf{F}(\mathbf{X}, t). \tag{24}$$

where $\mathbf{X} = (x_1, y_1, x_2, y_2)^{\mathrm{T}}$, and

$$\mathbf{F}\left(\mathbf{X}, t + \frac{2\pi}{\omega}\right) = \mathbf{F}(\mathbf{X}, t). \tag{25}$$

Eq. (5) can be rewritten as

$$\begin{aligned}
y_{1+} &= a y_{1-} + b y_{2-},\\
y_{2+} &= c y_{1-} + d y_{2-},
\end{aligned} \tag{26}$$

where $y_{i-} = \dot{x}_{i-}$, $y_{i+} = \dot{x}_{i+}$ $(i=1,2)$ denote the non-dimensional velocities of M_i before and after impacting, respectively.

The phase space of the vibro-impact system is

$$\mathbf{R}^4 \times \mathbf{S}^1 = \left\{(x_1, y_1, x_2, y_2, t)\middle|(x_1, y_1, x_2, y_2) \in \mathbf{R}^4, t \in \mathbf{S}^1\right\}, \tag{27}$$

where $\mathbf{S}^1$ is unit circle. And the Poincaré section is chosen as

$$\mathbf{\Pi}_1 = \left\{(x_1, y_1, x_2, y_2, t) \in \mathbf{R}^4 \times \mathbf{S}^1 \middle| x_1 - x_2 = -b_f\right\}. \tag{28}$$

Subsequently, we define a transformation $\mathbf{R}: \mathbf{R}^4 \times \mathbf{S}^1 \mapsto \mathbf{R}^4 \times \mathbf{S}^1$:

$$\mathbf{R}: (x_1, y_1, x_2, y_2, t) \mapsto \left(-x_1, -y_1, -x_2, -y_2, t + \frac{n\pi}{\omega}\right) \tag{29}$$

and a section:

$$\mathbf{\Pi}_2 = \left\{(x_1, y_1, x_2, y_2, t) \in \mathbf{R}^4 \times \mathbf{S}^1 \middle| x_1 - x_2 = b_f\right\}. \tag{30}$$

Due to $t \in \mathbf{S}^1$, we have

$$\mathbf{R}^2 = \mathbf{I} \tag{31}$$

and

$$\begin{aligned} \mathbf{R}\mathbf{\Pi}_1 &= \mathbf{\Pi}_2, \\ \mathbf{R}\mathbf{\Pi}_2 &= \mathbf{\Pi}_1. \end{aligned} \tag{32}$$

Where $\mathbf{I}$ is the identical transformation. According to Eqs. (23), (24) and (29), we obtain

$$\mathbf{R}\mathbf{F}(\mathbf{X}) = \mathbf{F}(\mathbf{R}\mathbf{X}). \tag{33}$$

Proposition 2. *If* $\mathbf{X}(\mathbf{X}_0,t)$ $(t = t_0 + \Delta t)$ *is the solution of Eq.* (23) *which set out from the starting point* $\mathbf{X}_0 = (x_{10}, y_{10}, x_{20}, y_{20}, t_0) \in \mathbf{\Pi}_1$, *and* $\mathbf{X}(\mathbf{X}_1, t + (n\pi/\omega))$ *is the solution of Eq.* (23) *which set out from the starting point* $\mathbf{X}_1 = \mathbf{R}\mathbf{X}_0 \in \mathbf{\Pi}_2$, *we have*

$$\mathbf{X}\left(\mathbf{X}_1, t + \frac{n\pi}{\omega}\right) = \mathbf{R}\mathbf{X}(\mathbf{X}_0, t). \tag{34}$$

Equivalently,

$$\mathbf{X}\left(\mathbf{R}\mathbf{X}_0, t_0 + \Delta t + \frac{n\pi}{\omega}\right) = \mathbf{R}\mathbf{X}(\mathbf{X}_0, t_0 + \Delta t). \tag{35}$$

Proof. According to Eq. (33), we have

$$\frac{\mathrm{d}}{\mathrm{d}t}\mathbf{R}\mathbf{X}(\mathbf{X}_0, t) = \mathbf{R}\dot{\mathbf{X}}(\mathbf{X}_0, t) = \mathbf{R}\mathbf{F}(\mathbf{X}(\mathbf{X}_0, t)) = \mathbf{F}(\mathbf{R}\mathbf{X}(\mathbf{X}_0, t)). \tag{36}$$

Then $\mathbf{R}\mathbf{X}(\mathbf{X}_0, t)$ is the solution of Eq. (23).

Furthermore,

$$\mathbf{R}\mathbf{X}(\mathbf{X}_0, t_0) = \mathbf{R}\mathbf{X}(\mathbf{X}_0, t_0 + \Delta t)\big|_{\Delta t = 0} = \mathbf{R}\mathbf{X}_0 = \mathbf{X}_1. \tag{37}$$

Then we prove Eqs. (34) and (35) according to the uniqueness theorem of solution. □

Supposing that it takes Δt_1 time for the solution starting from $\mathbf{X}_0 \in \mathbf{\Pi}_1$ to reach the section $\mathbf{\Pi}_2$, and it takes Δt_2 time for the solution starting from $\mathbf{X}_1 = \mathbf{R}\mathbf{X}_0 \in \mathbf{\Pi}_2$ to reach the section $\mathbf{\Pi}_1$, then we can consider Δt_1 and Δt_2 as the minimum positive roots of the following two equations, respectively:

$$x_2(\mathbf{X}_0, t_0 + \Delta t_1) - x_1(\mathbf{X}_0, t_0 + \Delta t_1) = -b_f, \tag{38}$$

$$x_2(\mathbf{X}_1, t_1 + \Delta t_2) - x_1(\mathbf{X}_1, t_1 + \Delta t_2) = +b_f, \tag{39}$$

where

$$\mathbf{X}_1 = \mathbf{R}\mathbf{X}_0 \tag{40}$$

and $t_1 = t_0 + (n\pi/\omega)$. According to Eqs. (36) and (37), Δt_1 and Δt_2 can be expressed as the following functions:

$$\begin{aligned} \Delta t_1 &= \Delta t_1(x_{10}, y_{10}, x_{20}, y_{20}, t_0), \\ \Delta t_2 &= \Delta t_2(x_{11}, y_{11}, x_{21}, y_{21}, t_1). \end{aligned} \tag{41}$$

Considering Eqs. (35) and (36), we obtain

$$\mathbf{R}(x_2(\mathbf{X}_0, t_0 + \Delta t_1) - x_1(\mathbf{X}_0, t_0 + \Delta t_1)) = x_2(\mathbf{X}_1, t_1 + \Delta t_1) - x_1(\mathbf{X}_1, t_1 + \Delta t_1) = +b_f. \tag{42}$$

According to Eqs. (37) and (40), we have

$$\Delta t_1 = \Delta t_2. \tag{43}$$

(y_1, x_2, y_2, t) are chosen as the coordinates of the Poincaré section. Supposing $\mathbf{Q}_1$ represents the map from $\mathbf{\Pi}_1$ to $\mathbf{\Pi}_2$, and $\mathbf{Q}_2$ represents the map from $\mathbf{\Pi}_2$ to $\mathbf{\Pi}_1$, and defining $\mathbf{Q}_1 : \mathbf{X}_0 \mapsto \mathbf{X}_1$, where

$$\begin{aligned} \mathbf{X}_0 &= (y_{10}, x_{20}, y_{20}, t_0) \in \mathbf{\Pi}_1, \\ \mathbf{X}_1 &= (y_{11}, x_{21}, y_{21}, t_1) \in \mathbf{\Pi}_2, \end{aligned} \tag{44}$$

we have

$$\begin{aligned} y_{11} &= a y_1(\mathbf{X}_0, t_0 + \Delta t_1) + b y_2(\mathbf{X}_0, t_0 + \Delta t_1), \\ x_{21} &= x_2(\mathbf{X}_0, t_0 + \Delta t_1), \\ y_{21} &= c y_1(\mathbf{X}_0, t_0 + \Delta t_1) + d y_2(\mathbf{X}_0, t_0 + \Delta t_1), \\ t_1 &= t_0 + \Delta t_1 \left(\mathrm{mod} \frac{2\pi}{\omega} \right). \end{aligned} \tag{45}$$

Defining $\mathbf{Q}_2 : \mathbf{X}_1 \mapsto \mathbf{X}_2$ where

$$\mathbf{X}_2 = (y_{12}, x_{22}, y_{22}, t_2) \in \mathbf{\Pi}_1, \tag{46}$$

we have

$$\begin{aligned} y_{12} &= a y_1(\mathbf{X}_1, t_1 + \Delta t_2) + b y_2(\mathbf{X}_1, t_1 + \Delta t_2), \\ x_{22} &= x_2(\mathbf{X}_1, t_1 + \Delta t_2), \\ y_{22} &= c y_1(\mathbf{X}_1, t_1 + \Delta t_2) + d y_2(\mathbf{X}_1, t_1 + \Delta t_2), \\ t_2 &= t_1 + \Delta t_2 \left(\mathrm{mod} \frac{2\pi}{\omega} \right). \end{aligned} \tag{47}$$

The Poincaré map can be given as

$$\mathbf{P} = \mathbf{Q}_2 \circ \mathbf{Q}_1, \quad \mathbf{P} : \mathbf{\Pi}_1 \mapsto \mathbf{\Pi}_1. \tag{48}$$

Proposition 3. *The Poincaré map has the symmetry property*:

$$\mathbf{R} \circ \mathbf{Q}_1 = \mathbf{Q}_2 \circ \mathbf{R}. \tag{49}$$

Proof. According to Eqs. (35) and (45), for $\mathbf{X}_0 \in \mathbf{\Pi}_1$, we have

$$\begin{aligned} &\mathbf{R} \circ \mathbf{Q}_1(\mathbf{X}_0) \\ &\quad = \mathbf{R}(a y_1(\mathbf{X}_0, t_0 + \Delta t_1) + b y_2(\mathbf{X}_0, t_0 + \Delta t_1), \quad x_2(\mathbf{X}_0, t_0 + \Delta t_1), \quad c y_1(\mathbf{X}_0, t_0 + \Delta t_1) \\ &\qquad + d y_2(\mathbf{X}_0, t_0 + \Delta t_1), t_0 + \Delta t_1) \\ &\quad = (a y_1(\mathbf{X}_1, t_1 + \Delta t_1) + b y_2(\mathbf{X}_1, t_1 + \Delta t_1), \quad x_2(\mathbf{X}_1, t_1 + \Delta t_1), \quad c y_1(\mathbf{X}_1, t_1 + \Delta t_1) \\ &\qquad + d y_2(\mathbf{X}_1, t_1 + \Delta t_1), t_1 + \Delta t_1). \end{aligned} \tag{50}$$

According to Eqs. (40) and (47), we obtain

$$\begin{aligned} &\mathbf{Q}_2 \circ \mathbf{R}(\mathbf{X}_0) \\ &\quad = \mathbf{Q}_2(\mathbf{X}_1) \\ &\quad = (a y_1(\mathbf{X}_1, t_1 + \Delta t_2) + b y_2(\mathbf{X}_1, t_1 + \Delta t_2), \quad x_2(\mathbf{X}_1, t_1 + \Delta t_2), \quad c y_1(\mathbf{X}_1, t_1 + \Delta t_2) \\ &\qquad + d y_2(\mathbf{X}_1, t_1 + \Delta t_2), \quad t_1 + \Delta t_2) \\ &\quad = \mathbf{R} \circ \mathbf{Q}_1(\mathbf{X}_0), \end{aligned} \tag{51}$$

such that Eq. (49) is proved. □

Eq. (49) can be rewritten as

$$\mathbf{Q}_2 = \mathbf{R} \circ \mathbf{Q}_1 \circ \mathbf{R}^{-1}. \tag{52}$$

Introducing a map

$$\mathbf{Q}_\alpha = \mathbf{R}^{-1} \circ \mathbf{Q}_1, \tag{53}$$

we obtain the Poincaré map follows:

$$\mathbf{P} = \mathbf{Q}_2 \circ \mathbf{Q}_1 = \mathbf{R} \circ \mathbf{Q}_1 \circ \mathbf{R}^{-1} \circ \mathbf{Q}_1 = \mathbf{R}^2 \circ (\mathbf{R}^{-1} \circ \mathbf{Q}_1) = \mathbf{Q}_\alpha^2. \tag{54}$$

5. Stability and bifurcations

If $\mathbf{X}_0 \in \mathbf{\Pi}_1$ satisfies $\mathbf{P}(\mathbf{X}_0) = \mathbf{X}_0$, then $\mathbf{X}_0$ is a fixed point of the Poincaré map $\mathbf{P}$. If the fixed point $\mathbf{X}_0$ satisfies

$$\mathbf{X}_0 = \mathbf{R}^{-1} \circ \mathbf{Q}_1(\mathbf{X}_0), \tag{55}$$

then $\mathbf{X}_0$ is said to be a symmetric fixed point of $\mathbf{P}$.

Proposition 4. *If $\mathbf{X}_\alpha$ is a fixed point of the Poincaré map, and*

$$\mathbf{X}_\beta = \mathbf{R}^{-1} \circ \mathbf{Q}_1(\mathbf{X}_\alpha) \neq \mathbf{X}_\alpha, \tag{56}$$

then $\mathbf{X}_\beta$ is also the fixed point of the Poincaré map, and $\mathbf{X}_\alpha$ and $\mathbf{X}_\beta$ have the same stability ($\mathbf{X}_\alpha$ and $\mathbf{X}_\beta$ are said to be a pair of antisymmetric fixed point which corresponds to a pair of antisymmetric period $n-2$ motions).

Proof. Substituting formula (50) into Eq. (48), we have

$$\begin{aligned}\mathbf{P}(\mathbf{X}_\beta) &= \mathbf{Q}_\alpha^2(\mathbf{X}_\beta) = (\mathbf{R}^{-1} \circ \mathbf{Q}_1)^2(\mathbf{X}_\beta) = (\mathbf{R}^{-1} \circ \mathbf{Q}_1) \circ (\mathbf{R}^{-1} \circ \mathbf{Q}_1)^2(\mathbf{X}_\alpha) \\ &= (\mathbf{R}^{-1} \circ \mathbf{Q}_1)(\mathbf{X}_\alpha) = \mathbf{X}_\beta,\end{aligned} \tag{57}$$

then $\mathbf{X}_\beta$ is also the fixed point of the Poincaré map, and

$$\mathbf{DP}(\mathbf{X}_\alpha) = \mathbf{D}(\mathbf{R}^{-1} \circ \mathbf{Q}_1)(\mathbf{X}_\beta)\mathbf{D}(\mathbf{R}^{-1} \circ \mathbf{Q}_1)(\mathbf{X}_\alpha) = \mathbf{BA}, \tag{58}$$

$$\mathbf{DP}(\mathbf{X}_\beta) = \mathbf{D}(\mathbf{R}^{-1} \circ \mathbf{Q}_1)(\mathbf{X}_\alpha)\mathbf{D}(\mathbf{R}^{-1} \circ \mathbf{Q}_1)(\mathbf{X}_\beta) = \mathbf{AB}, \tag{59}$$

where

$$\mathbf{A} = \mathbf{D}(\mathbf{R}^{-1} \circ \mathbf{Q}_1)(\mathbf{X}_\alpha), \tag{60}$$

$$\mathbf{B} = \mathbf{D}(\mathbf{R}^{-1} \circ \mathbf{Q}_1)(\mathbf{X}_\beta). \tag{61}$$

Due to $\det \mathbf{A} \neq 0$ for nondegenerate fixed point, we have

$$\mathbf{BA} = \mathbf{A}^{-1}(\mathbf{AB})\mathbf{A}. \tag{62}$$

Equivalently,

$$\mathbf{DP}(\mathbf{X}_\alpha) = \mathbf{A}^{-1}(\mathbf{DP}(\mathbf{X}_\beta))\mathbf{A}, \tag{63}$$

then $\mathbf{DP}(\mathbf{X}_\alpha)$ is similar to $\mathbf{DP}(\mathbf{X}_\beta)$, and both the Jacobian matrices of $\mathbf{X}_\alpha$ and $\mathbf{X}_\beta$ have the same set of eigenvalues. Hence, we arrive the conclusion that the two antisymmetric fixed points $\mathbf{X}_\alpha$ and $\mathbf{X}_\beta$ have the same stability. □

6. Computation of the Jacobian matrix

At the instant after impacting, the non-dimensional time is always set to zero, and the phase angle has a corresponding change at the same time. So the coordinates (y_{10}, x_{20}, y_{20}, t_0) of the fixed point are translated into (y_{10}, x_{20}, y_{20}, τ_0) in the following computation.

The Poincaré map is a composition of following four sub-maps: (I) The map from the instant after impacting at the right stop ($t = 0$) to the instant before impacting at the left stop ($t = t_1$). (II) The map of impacting at the left stop ($t = t_1$). (III) The map from the instant after impacting at the left stop ($t = t_1$) to the instant before impacting at the right stop ($t = t_2$). (IV) The map of impacting at the right stop ($t = t_2$). The four sub-maps above can be expressed follows:

$$\begin{aligned}
&\mathbf{P}_1 : (\dot{x}_{1+}(0), x_2(0), \dot{x}_{2+}(0), \tau(0)) \mapsto (\dot{x}_{1-}(t_1), x_2(t_1), \dot{x}_{2-}(t_1), \tau(t_1)),\\
&\mathbf{P}_2 : (\dot{x}_{1-}(t_1), x_2(t_1), \dot{x}_{2-}(t_1), \tau(t_1)) \mapsto (\dot{x}_{1+}(t_1), x_2(t_1), \dot{x}_{2+}(t_1), \tau(t_1)),\\
&\mathbf{P}_3 : (\dot{x}_{1+}(t_1), x_2(t_1), \dot{x}_{2+}(t_1), \tau(t_1) \mapsto (\dot{x}_{1-}(t_2), x_2(t_2), \dot{x}_{2-}(t_2), \tau(t_2)),\\
&\mathbf{P}_4 : (\dot{x}_{1-}(t_2), x_2(t_2), \dot{x}_{2-}(t_2), \tau(t_2)) \mapsto (\dot{x}_{1+}(t_2), x_2(t_2), \dot{x}_{2+}(t_2), \tau(t_2)).
\end{aligned} \tag{64}$$

Let $\mathbf{DP}_1$, $\mathbf{DP}_2$, $\mathbf{DP}_3$ and $\mathbf{DP}_4$ represent the linearized matrices of sub-maps $\mathbf{P}_1$, $\mathbf{P}_2$, $\mathbf{P}_3$ and $\mathbf{P}_4$, respectively:

$$\begin{aligned}
\mathbf{DP}_1 &= \begin{bmatrix} a_{11} & a_{12} & a_{13} & a_{14} \\ a_{21} & a_{22} & a_{23} & a_{24} \\ a_{31} & a_{32} & a_{33} & a_{34} \\ a_{41} & a_{42} & a_{43} & a_{44} \end{bmatrix}, \quad \mathbf{DP}_2 = \begin{bmatrix} b_{11} & b_{12} & b_{13} & b_{14} \\ b_{21} & b_{22} & b_{23} & b_{24} \\ b_{31} & b_{32} & b_{33} & b_{34} \\ b_{41} & b_{42} & b_{43} & b_{44} \end{bmatrix},\\
\mathbf{DP}_3 &= \begin{bmatrix} c_{11} & c_{12} & c_{13} & c_{14} \\ c_{21} & c_{22} & c_{23} & c_{24} \\ c_{31} & c_{32} & c_{33} & c_{34} \\ c_{41} & c_{42} & c_{43} & c_{44} \end{bmatrix}, \quad \mathbf{DP}_4 = \begin{bmatrix} d_{11} & d_{12} & d_{13} & d_{14} \\ d_{21} & d_{22} & d_{23} & d_{24} \\ d_{31} & d_{32} & d_{33} & d_{34} \\ d_{41} & d_{42} & d_{43} & d_{44} \end{bmatrix}.
\end{aligned} \tag{65}$$

The Poincaré map can be expressed as

$$\mathbf{P} = \mathbf{P}_4 \circ \mathbf{P}_3 \circ \mathbf{P}_2 \circ \mathbf{P}_1 : (\dot{x}_{1+}(0), x_2(0), \dot{x}_{2+}(0), \tau(0)) \mapsto (\dot{x}_{1+}(t_2), x_2(t_2), \dot{x}_{2+}(t_2), \tau(t_2)) \tag{66}$$

and its Jacobian matrix can be expressed as

$$\mathbf{DP} = \mathbf{DP}_4\mathbf{DP}_3\mathbf{DP}_2\mathbf{DP}_1. \tag{67}$$

For maps (II) and (IV), we have the following formula according to the impact law:

$$\mathbf{DP}_2 = \mathbf{DP}_4 = \begin{bmatrix} a & 0 & b & 0 \\ 0 & 1 & 0 & 0 \\ c & 0 & d & 0 \\ 0 & 0 & 0 & 1 \end{bmatrix} \tag{68}$$

and for map (I), we have

$$\mathbf{DP}_1(\mathbf{X}_0) = \left[\frac{\partial P_{1i}}{\partial X_{0j}}\right]\Bigg|_{(\dot{x}_{10}, x_{20}, \dot{x}_{20}, \tau_0)}, \quad i,j = 1,2,3,4, \tag{69}$$

where X_{0j} denote the coordinates $(\dot{x}_{10}, x_{20}, \dot{x}_{20}, \tau_0)$, respectively, and P_{1i} is the component of $\mathbf{P}_1(\mathbf{X}_0)$ given as follows:

$$\begin{aligned}
\dot{x}_1' &= \mathrm{e}^{-\zeta t_1}(A_1(-\zeta \cos(\omega_{d1} t_1) - \omega_{d1} \sin(\omega_{d1} t_1)) + A_2(-\zeta \sin(\omega_{d1} t_1) + \omega_{d1} \cos(\omega_{d1} t_1)))\\
&\quad + B_1\omega \cos(\omega t_1 + \tau_0) - B_2\omega \sin(\omega t_1 + \tau_0)\\
&= P_{11}(\mathbf{X}_0),
\end{aligned} \tag{70a}$$

$$\begin{aligned}
x_2' &= \mathrm{e}^{-\eta t_1}(A_3 \cos(\omega_{d2} t_1) + A_4 \sin(\omega_{d2} t_1)) + B_3 \sin(\omega t_1 + \tau_0) + B_4 \cos(\omega t_1 + \tau_0)\\
&= P_{12}(\mathbf{X}_0),
\end{aligned} \tag{70b}$$

$$\dot{x}_2' = e^{-\eta t_1}(A_3(-\eta \cos(\omega_{d2} t_1) - \omega_{d2} \sin(\omega_{d2} t_1)) + A_4(-\eta \sin(\omega_{d2} t_1) + \omega_{d2} \cos(\omega_{d2} t_1))) + B_3\omega \cos(\omega t_1 + \tau_0) - B_4\omega \sin(\omega t_1 + \tau_0) = P_{13}(\mathbf{X}_0), \tag{70c}$$

$$\tau' = \omega t_1 + \tau_0 = P_{14}(\mathbf{X}_0), \tag{70d}$$

where the function $t_1 = t_1(\dot{x}_{10}, x_{20}, \dot{x}_{20}, \tau_0)$ is the solution of the following equation:

$$G(t_1, \dot{x}_{10}, x_{20}, \dot{x}_{20}, \tau_0) = e^{-\eta t_1}(A_3 \cos(\omega_{d2} t_1) + A_4 \sin(\omega_{d2} t_1)) + B_3 \sin(\omega t_1 + \tau_0) + B_4 \cos(\omega t_1 + \tau_0) - e^{-\zeta t_1}(A_1 \cos(\omega_{d1} t_1) + A_2 \sin(\omega_{d1} t_1)) - B_1 \sin(\omega t_1 + \tau) - B_2 \cos(\omega t_1 + \tau) - b_f = 0. \tag{71}$$

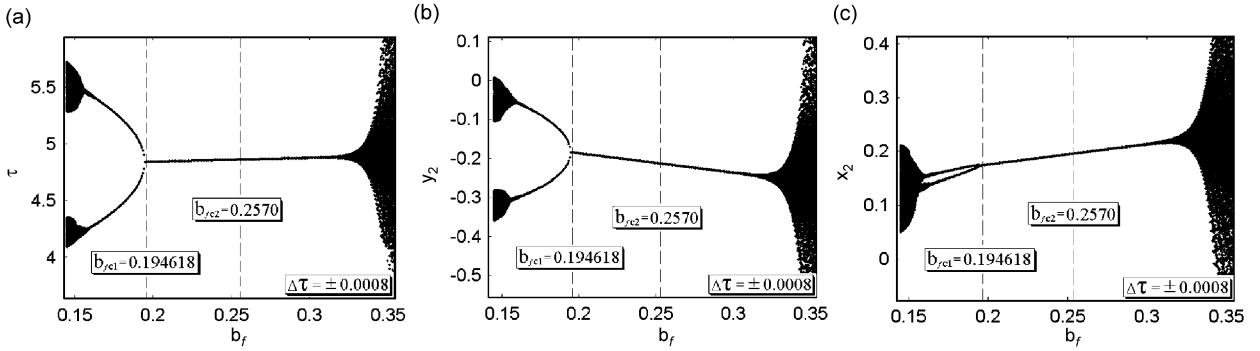

Fig. 2. The bifurcation diagrams: $u_m = 1.5$, $u_c = 1$, $u_k = 1$, $\zeta = 0.0001$, $f_2 = 0.2$, $R = 0.8$, $\omega = 2.2$: (a) b_f–τ, (b) b_f–y_2 and (c) b_f–x_2.

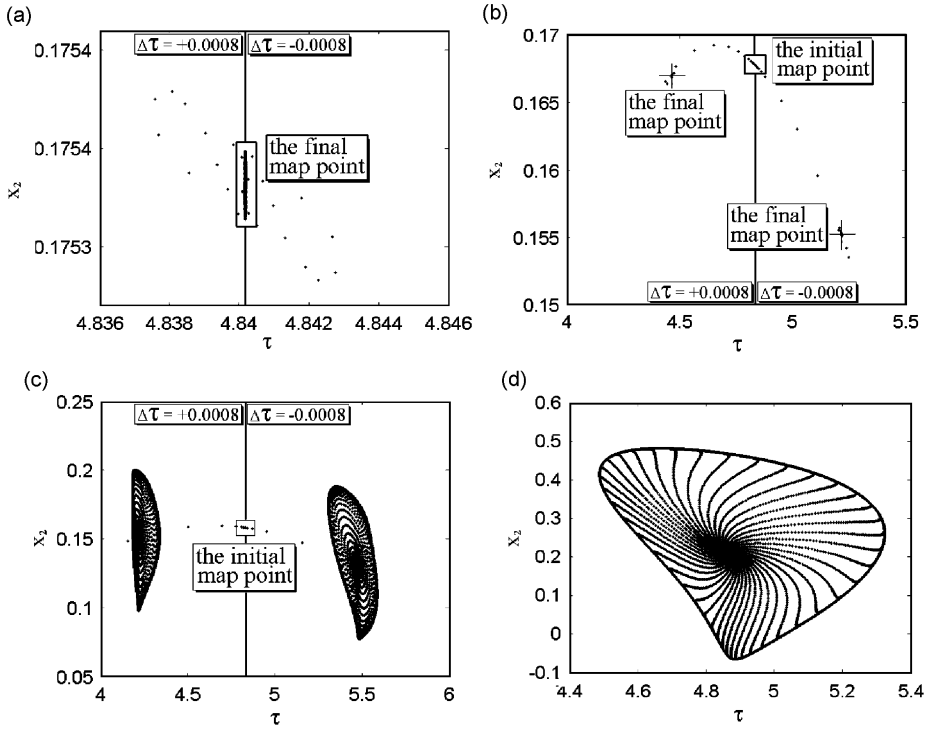

Fig. 3. On the coordinate plane (τ, x_2): (a) $b_f = 0.2$, (b) $b_f = 0.18$, (c) $b_f = 0.155$ and (d) $b_f = 0.285$.

Considering Eqs. (69) and (70), we can obtain the entries of the matrix $\mathbf{DP}_1$ (see Appendix B) using the implicit function theorem. Subsequently, we can obtain the entries of the matrix $\mathbf{DP}_3$ by replacing $(\dot{x}_{10}, x_{20}, \dot{x}_{20}, \tau_0)$ in $\mathbf{DP}_1$ with $(-\dot{x}_{10}, -x_{20}, -\dot{x}_{20}, \tau_0 + n\pi)$.

7. Numerical simulations

7.1. Bifurcations with the first set of system parameters

The vibro-impact system with parameters: (1) $u_m = 1.5$, $u_c = 1$, $u_k = 1$, $\zeta = 0.0001$, $f_2 = 0.2$, $R = 0.8$, $\omega = 2.2$, have been chosen for analysis, and the non-dimensional clearance b_f is taken as a control parameter. All eigenvalues of $\mathbf{DP}(\mathbf{X}_0)$ are computed and listed in Appendix C. With $b_f = b_{fc1} = 0.194618$, there is a real eigenvalue of $+1$, and the other three eigenvalues lie inside the unit circle, so b_{fc1} is the critical parameter value of pitchfork bifurcation. As b_f increases to $b_f = b_{fc2} = 0.2570$, there is a pair of complex conjugate eigenvalues crossing the unit circle, and the moduli of the other pair of complex conjugate eigenvalues is less than 1, hence b_{fc2} is the critical parameter value of Hopf bifurcations.

Bifurcation diagrams are shown in Fig. 2. Indeed, we can find that $b_f = b_{fc1} = 0.194618$ is the critical parameter value of pitchfork bifurcation, and $b_f = b_{fc2} = 0.2570$ is the critical parameter value of Hopf

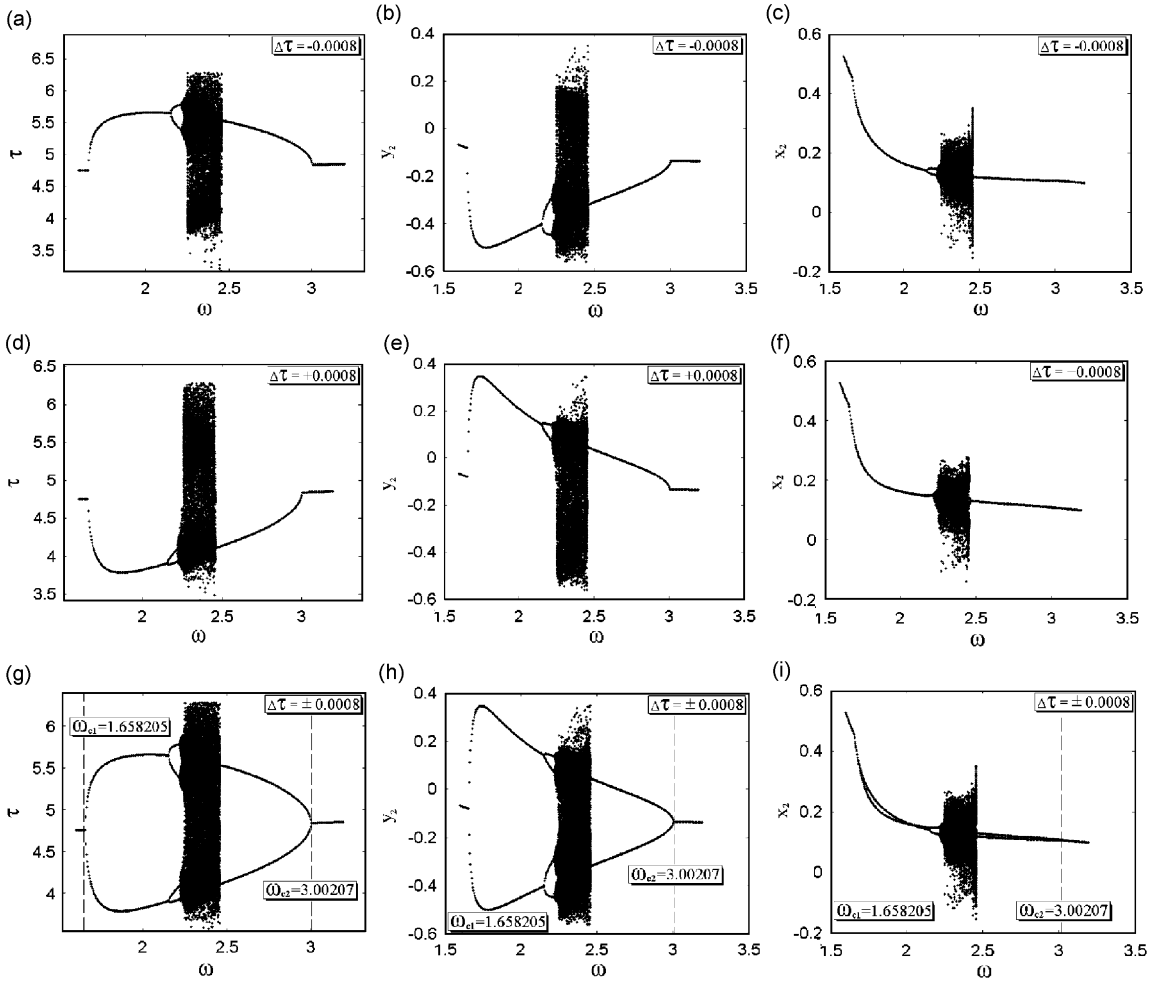

Fig. 4. The bifurcation diagrams: $u_m = 1$, $u_c = 1$, $u_k = 2$, $\zeta = 0.0001$, $f_2 = 0.2$, $R = 0.8$, $b_f = 0.08$: (a)–(c): $\Delta\tau_0 = -0.0008$; (e)–(f): $\Delta\tau_0 = +0.0008$ and (g)–(i) $\Delta\tau = \pm 0.0008$.

bifurcation. There is a stable symmetric fixed point of the Poincaré map for $b_f \in \lfloor b_{fc1}, b_{fc2} \rfloor$. If $b_f < b_{fc1}$, pitchfork bifurcation takes place. If $b_f > b_{fc2}$, Hopf bifurcation occurs.

The projections of Poincaré map on the coordinate plane (τ, x_2) are represented in Fig. 3. In Fig. 3(a), it is shown that the Poincaré map has a stable symmetric fixed point (4.8402,0.1754) with $b_f = 0.2 \in \lfloor b_{fc1}, b_{fc2} \rfloor$. With $b_f = 0.18 < b_{fc1}$, pitchfork bifurcation has taken place. We can compute one unstable symmetric fixed point (4.8333,0.1678) when $b_f = 0.18 < b_{fc1}$. If we add a small perturbations $\Delta\tau = \pm 0.0008$ to the unstable fixed point (4.8333,0.1678), respectively, we obtain two initial points. Iterate the two initial points, respectively, we reach two stable antisymmetric fixed points (4.4654,0.1670) and (5.2174,0.1552), see Fig. 3(b). As b_f decreases to $b_f = 0.155$, the two stable antisymmetric fixed points are transformed into two Hopf circles, respectively, as shown in Fig. 3(c). However, with $b_f = 0.285 < b_{fc2}$, there will be Hopf bifurcation of the symmetric fixed point, as shown in Fig. 3(d).

7.2. Bifurcations with the second set of system parameters

7.2.1. Eigenvalues of the Jacobian matrix

The vibro-impact system with parameters: (1) $u_m = 1$, $u_c = 1$, $u_k = 2$, $\zeta = 0.0001$, $f_2 = 0.2$, $R = 0.8$, $b_f = 0.08$, are considered, and the frequency ω is taken as a control parameter. The eigenvalues of the Jacobian matrix are computed for $\omega \in [1.65, 3.5]$. All the eigenvalues and their moduli are listed in Appendix D. The stability and bifurcations of the fixed point can be determined by the moduli of the eigenvalues.

With $\omega = \omega_{c1} = 1.658205$, there is a real eigenvalue of $+1$, and the other three eigenvalues lie inside the unit circle, then ω_{c1} is the critical parameter value of pitchfork bifurcation, so is $\omega = \omega_{c2} = 3.00207$. When $\omega = 1.6500 < \omega_{c1}$, all eigenvalues lie inside the unit circle, hence the symmetric fixed point is stable. However, with $\omega \in [\omega_{c1}, \omega_{c2}]$, there is a real eigenvalue being outside the unit circle, and the remainders of the eigenvalues are strictly inside the unit circle. Then there will be two antisymmetric fixed points bifurcated from the symmetric fixed point via pitchfork bifurcation.

With $\omega \in [\omega_{c2}, \omega_{c3}]$, all eigenvalues lie inside the unit circle and the fixed point is stable. However, as ω increases and passes through $\omega = \omega_{c3} = 3.4205$, there is a pair of complex conjugate eigenvalues crossing the unit circle, and the moduli of the other pair of complex conjugate eigenvalues are less than 1, so ω_{c3} is the

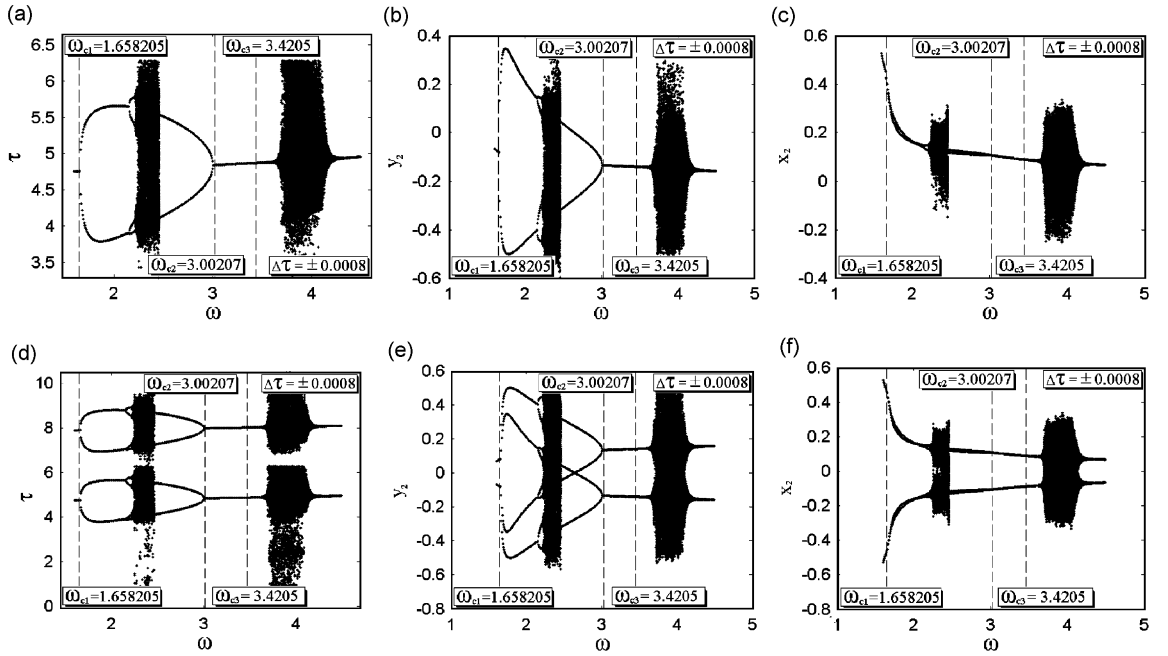

Fig. 5. The bifurcation diagrams: $u_m = 1$, $u_c = 1$, $u_k = 2$, $\zeta = 0.0001$, $f_2 = 0.2$, $r = 0.8$, $b_f = 0.08$: (a)–(c) Diagrams on the Poincaré section $\mathbf{\Pi}_1$; (d)–(f) diagrams on both $\mathbf{\Pi}_1$ and $\mathbf{\Pi}_2$.

critical parameter value of Hopf bifurcation. With further increasing parameter ω, there will be a Hopf circle bifurcated from the symmetric fixed point.

7.2.2. *Bifurcation diagrams*

The bifurcation diagrams as $\omega \in [1.6, 3.2]$ are represented in Fig. 4. Let the initial perturbation be $\Delta\tau_0 = -0.0008$, we obtain the bifurcation diagrams Figs. 4(a)–(c). With $\Delta\tau_0 = +0.0008$, the bifurcation diagrams are Figs. 4(d)–(f). If the two cases above are considered at the same time, the bifurcation diagrams are Figs. 4(g)–(i).

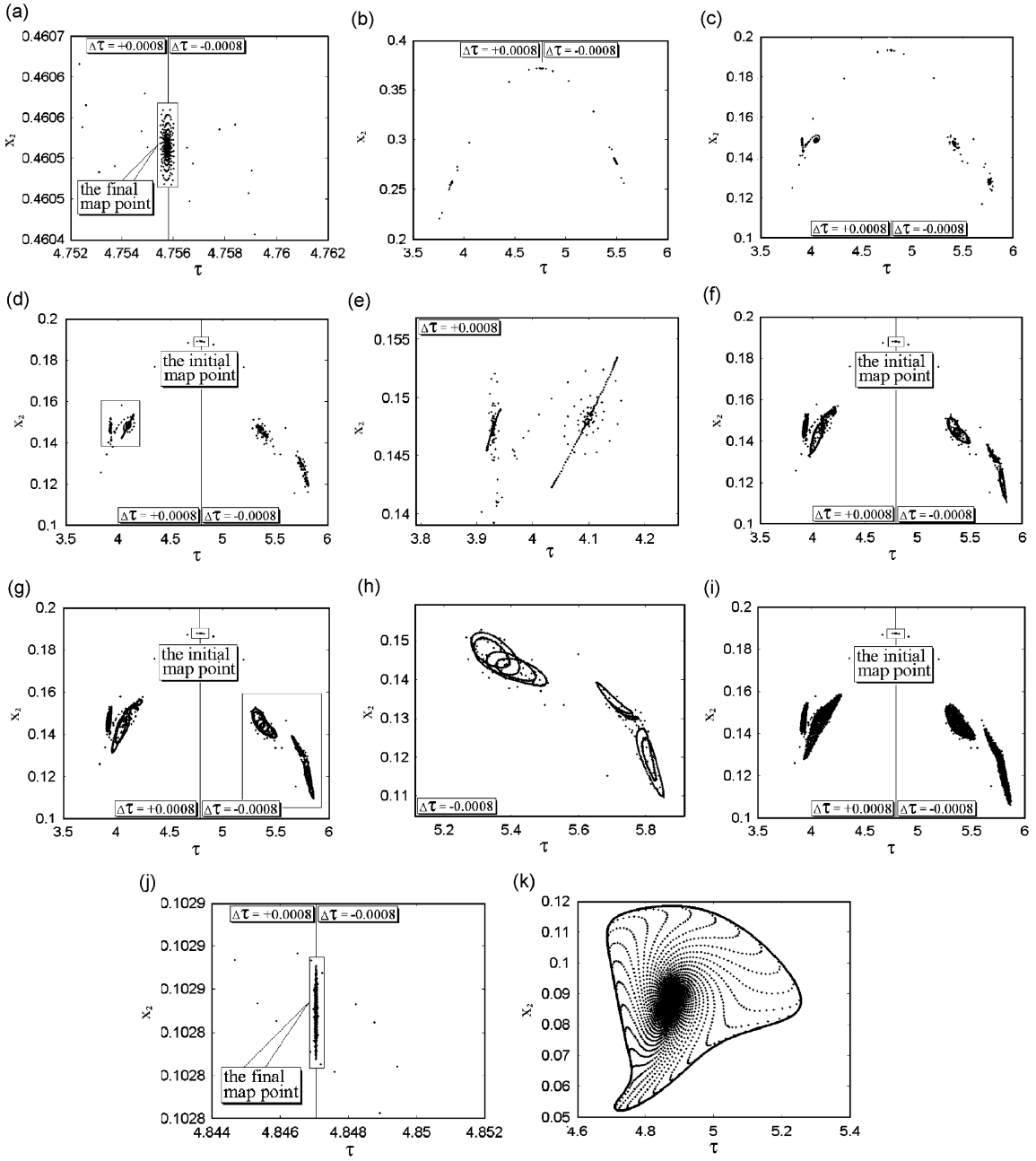

Fig. 6. On the coordinate plane (τ, x_2): (a) $\omega = 1.65$, (b) $\omega = 1.745$, (c) $\omega = 2.2$, (d), (e) $\omega = 2.22$, (f) $\omega = 2.226$, (g) $\omega = 2.227$, (h), (i) $\omega = 2.229$, (j) $\omega = 3.1$ and (k) $\omega = 3.5$.

As Figs. 4(g)–(i), $\omega = \omega_{c1} = 1.658205$ is the critical parameter value of the pitchfork bifurcation indeed. When $\omega \in [\omega_{c1},\omega_{c2}]$, there may be two antisymmetric fixed points, and both of them are stable.

It should be noted that the system settles into chaotic motion via period-doublng bifurcations nearby $\omega = 2.3$. However, the Poincaré map resumes two stable antisymmetric fixed points for $\omega > 2.405$. When ω increases to $\omega = \omega_{c2} = 3.00207$, the duration of pitchfork bifurcations ended, and the Poincaré map has only one stable symmetric fixed point with $\omega \in [\omega_{c2},\omega_{c3}]$.

The bifurcation diagrams with $\omega \in [1.6,4.5]$ are represented in Fig. 5. Figs. 5(a)–(c) show the bifurcation diagrams on $\mathbf{\Pi}_1$, and Figs. 5(d)–(f) represent the bifurcation diagrams on both $\mathbf{\Pi}_1$ and $\mathbf{\Pi}_2$. The symmetric fixed point is stable with $\omega \in [1.61,\omega_{c1}]$, and pitchfork bifurcation takes place with $\omega \in [\omega_{c1},\omega_{c2}]$. The symmetric fixed point restores the stable property with $\omega \in [\omega_{c2},\omega_{c3}]$. However, with $\omega > \omega_{c3}$, there may be a Hopf circle bifurcated from the symmetric fixed point. It should be mentioned that the bifurcation diagram on $\mathbf{\Pi}_1$ and on $\mathbf{\Pi}_2$ are exactly symmetric, see Figs. 5(d)–(f).

7.2.3. Phase diagrams

The phase diagrams on the coordinate plane (τ, x_2) are represented in Fig. 6. As seen in Fig. 6(a), whether the initial perturbation be $\Delta\tau_0 = -0.0008$ or 0.0008, we can obtain a stable fixed point (4.7558,0.4606). However, when ω increases and goes beyond $\omega = \omega_{c1} = 1.658205$, pitchfork bifurcation takes place. For example, the coordinates of the unstable symmetric fixed point are (4.7627,0.3718) with $\omega = 1.745$. If we add a perturbation $\Delta\tau = -0.0008$ to this point and iterate it, we obtain one stable antisymmetric fixed point (5.4926,0.2785). However, If we add a perturbation $\Delta\tau = +0.0008$ to the initial point, we obtain another stable antisymmetric fixed point (3.8834,0.2564), see Fig. 6(b). As ω increases to $\omega = 2.2$, both of the two stable antisymmetric orbits undergo the first period-doubling bifurcation simultaneously, and the second period-doubling bifurcation takes place simultaneously nearby $\omega = 2.22$, see Figs. 6(c)–(d). Fig. 6(e) is a local magnification to Fig. 6(c). When ω increases to $\omega = 2.226$, the four stable fixed points are transformed into four Hopf circles, see Fig. 6(f). With further increasing ω, the non-periodic motion, or chaos will occur via the Hopf circle doubling, as shown in Figs. 6(g)–(i). Fig. 6(h) is a local magnification to Fig. 6(g).

When ω increases to $\omega = \omega_{c2} = 3.00207$, the duration of the pitchfork bifurcation ended, and the Poincaré section has only one stable symmetric fixed point with $\omega \in [\omega_{c2},\omega_{c3}]$. For example, a stable symmetric fixed point (4.8471,0.1029) can be obtained whether the initial perturbation $\Delta\tau_0 = -0.0008$ or $\Delta\tau_0 = 0.0008$ is chosen with $\omega = 3.1 \in [\omega_{c2},\omega_{c3}]$, see Fig. 6(j). However, as ω increases and passes through $\omega = \omega_{c3} = 3.4205$, Hopf bifurcation of the symmetric fixed point takes place, and Fig. 6(k) represents a Hopf circle bifurcated from the symmetric fixed point for $\omega = 3.5$.

8. Conclusions

In this paper, a two-degree-of-freedom vibro-impact system with symmetry is considered. The symmetric period $n-2$ motion and the Poincaré map of the system are derived analytically, and the symmetry of the Poincaré map is studied. It is shown that one symmetric fixed point may bifurcate into two antisymmetric fixed points, which have the same stability via pitchfork bifurcation. And the two antisymmetric fixed points correspond to two antisymmetric periodic motions of the system, respectively.

The numerical simulation shows that there may be pitchfork bifurcations and Hopf bifurcations in the two-degree-of-freedom vibro-impact system. If the Jacobian matrix of the Poincaré map has a real eigenvalue crossing the unit circle at $+1$, the symmetric fixed point could be transformed into two antisymmetric fixed points via pitchfork bifurcation, and both of them have the same stability. While the control parameter of the system changes continuously, the two antisymmetric fixed points will give birth to two synchronous bifurcation sequences, respectively.

For the symmetric fixed point, it may be a very special case that period-doubling bifurcations takes place. Both pitchfork bifurcations and Hopf bifurcations of the symmetric fixed point have been observed frequently, but period-doubling bifurcations of the symmetric fixed point have not been obtained yet.

Acknowledgments

This work was supported by the National Natural Science Foundation of China (10772151, 10472096) and Fund for Doctoral innovation of Southwest Jiaotong University.

Appendix A. The phase angle and the integration constants

$$\tau_0 = 2\tan^{-1}\left(\frac{u_1w_2 - u_2w_1 \pm \sqrt{(u_1w_2 - u_2w_1)^2 + (l_1w_2 - l_2w_1)^2 - (w_1v_2 - w_2v_1)^2 b_f^2}}{l_1w_2 - l_2w_1 + (w_2v_1 - w_1v_2)b_f}\right), \tag{A.1}$$

$$\begin{aligned} &A_1 = \frac{l_1c_0 + u_1s_0 - v_1b_f}{w_1} = \frac{l_2c_0 + u_2s_0 - v_2b_f}{w_2}, \quad A_2 = pA_1, \\ &A_3 = A_1 + (B_1 - B_3)s_0 + (B_2 - B_4)c_0 + b_f, \quad A_4 = qA_3, \end{aligned} \tag{A.2}$$

where

$$\begin{aligned} &s_0 = \sin(\tau_0), \quad c_0 = \cos(\tau_0), \quad s_1 = \sin\left(\frac{n\pi\omega_{d1}}{\omega}\right), \\ &c_1 = \cos\left(\frac{n\pi\omega_{d1}}{\omega}\right), \quad s_2 = \sin\left(\frac{n\pi\omega_{d2}}{\omega}\right), \quad c_2 = \cos\left(\frac{n\pi\omega_{d2}}{\omega}\right), \end{aligned} \tag{A.3}$$

$$\begin{aligned} w_1 &= \zeta - p\omega_{d1} + ae_1(h_1 - ph_2) + be_2(h_3 - h_4q), \\ w_2 &= \eta - q\omega_{d2} + ce_1(h_1 - ph_2) + de_2(h_3 - h_4q), \\ l_1 &= (-a + 1)B_1\omega - bB_3\omega + be_2(-h_3 + h_4q)(B_2 - B_4), \\ l_2 &= (-d + 1)B_3\omega - cB_1\omega + (-\eta + q\omega_{d2} + de_2(-h_3 + h_4q))(B_2 - B_4), \\ u_1 &= (-1 + a)B_2\omega + bB_4\omega + be_2(-h_3 + h_4q)(B_1 - B_3), \\ u_2 &= (-1 + d)B_4\omega + cB_2\omega + (-\eta + q\omega_{d2} + de_2(-h_3 + h_4q))(B_1 - B_3), \\ v_1 &= be_2(h_3 - h_4q), \quad v_2 = \eta - q\omega_{d2} + de_2(h_3 - h_4q), \end{aligned} \tag{A.4}$$

where

$$\begin{aligned} &p = -\frac{1 + e_1c_1}{e_1s_1}, \quad q = -\frac{1 + e_2c_2}{e_2c_2}, \quad e_1 = \mathrm{e}^{-\zeta(n\pi/\omega)}, \quad e_2 = \mathrm{e}^{-\eta(n\pi/\omega)}, \\ &h_1 = \zeta c_1 + \omega_{d1}s_1, \quad h_2 = -\zeta s_1 + \omega_{d1}c_1, \quad h_3 = \eta c_2 + \omega_{d2}s_2, \quad h_4 = -\eta s_2 + \omega_{d2}c_2. \end{aligned} \tag{A.5}$$

Appendix B. The entries of the matrix DP_1

$$\begin{aligned} a_{11} &= \frac{1}{\omega_{d1}}\mathrm{e}^{-\zeta t_1}(-\zeta\,\sin(\omega_{d1}t_1) + \omega_{d1}\,\cos(\omega_{d1}t_1)) + p_1\left(-\frac{q_1}{h}\right), \\ a_{12} &= \mathrm{e}^{-\zeta t_1}\left((-\zeta\,\cos(\omega_{d1}t_1) - \omega_{d1}\,\sin(\omega_{d1}t_1)) + \frac{\zeta}{\omega_{d1}}(-\zeta\,\sin(\omega_{d1}t_1) + \omega_{d1}\,\cos(\omega_{d1}t_1))\right) \\ &\quad + p_1\left(-\frac{q_2}{h}\right), \\ a_{13} &= p_1\left(-\frac{q_3}{h}\right), \\ a_{14} &= \mathrm{e}^{\zeta t_1}((-B_1c_0 + B_2s_0)(-\zeta\,\cos(\omega_{d1}t_1) - \omega_{d1}\,\sin(\omega_{d1}t_1) \\ &\quad + \frac{1}{\omega_{d1}}((-\zeta B_1 + \omega B_2)c_0 + (\zeta B_2 + \omega B_1)s_0)(-\zeta\,\sin(\omega_{d1}t_1) + \omega_{d1}\,\cos(\omega_{d1}t_1))) \\ &\quad - B_1\omega\,\sin(\omega t_1 + \tau_0) - B_2\omega\,\cos(\omega t_1 + \tau_0) + p_1\left(-\frac{q_4}{h}\right), \end{aligned} \tag{B.1}$$

$$
\begin{aligned}
a_{21} &= p_2\Big(-\frac{q_1}{h}\Big),\\
a_{22} &= \mathrm{e}^{-\eta t_1}\left(\cos(\omega_{d2}t_1)+\frac{\eta}{\omega_{d2}}\sin(\omega_{d2}t_1)\right)+p_2\Big(-\frac{q_2}{h}\Big),\\
a_{23} &= \frac{1}{\omega_{d2}}\mathrm{e}^{-\eta t_1}\sin(\omega_{d2}t_1)+p_2\Big(-\frac{q_3}{h}\Big),\\
a_{24} &= \mathrm{e}^{-\eta t_1}\Bigg(\left(-B_3c_0+B_4s_0\right)\cos(\omega_{d2}t_1)+\frac{1}{\omega_{d2}}((-\eta B_3+\omega B_4)c_0\\
&\quad +(\eta B_4+\omega B_3)s_0)\sin(\omega_{d2}t_1))+B_3\cos(\omega t_1+\tau_0)-B_4\sin(\omega t_1+\tau_0)+p_2\Big(-\frac{q_4}{h}\Big),
\end{aligned}
\tag{B.2}
$$

$$
\begin{aligned}
a_{31} &= p_3\Big(-\frac{q_1}{h}\Big),\\
a_{32} &= \mathrm{e}^{-\eta t_1}\left((-\eta\cos(\omega_{d2}t_1)-\omega_{d2}\sin(\omega_{d2}t_1))+\frac{\eta}{\omega_{d2}}(-\eta\sin(\omega_{d2}t_1)+\omega_{d2}\cos(\omega_{d2}t_1))\right)+p_3\Big(-\frac{q_2}{h}\Big),\\
a_{33} &= \frac{1}{\omega_{d2}}\mathrm{e}^{-\eta t_1}(-\eta\sin(\omega_{d2}t_1)+\omega_{d2}\cos(\omega_{d2}t_1))+p_3\Big(-\frac{q_3}{h}\Big),\\
a_{34} &= \mathrm{e}^{\eta t_1}((-B_3c_0+B_4s_0)(-\eta\cos(\omega_{d2}t_1)-\omega_{d2}\sin(\omega_{d2}t_1)\\
&\quad +\frac{1}{\omega_{d2}}((-\eta B_3+\omega B_4)c_0+(\eta B_4+\omega B_3)s_0)(-\eta\sin(\omega_{d2}t_1)+\omega_{d2}\cos(\omega_{d2}t_1))\Big)\\
&\quad -B_3\omega\sin(\omega t_1+\tau_0)-B_4\omega\cos(\omega t_1+\tau_0)+p_3\Big(-\frac{q_4}{h}\Big),
\end{aligned}
\tag{B.3}
$$

$$
a_{41}=-\frac{q_1}{h}\omega,\quad a_{42}=-\frac{q_2}{h}\omega,\quad a_{43}=-\frac{q_3}{h}\omega,\quad a_{44}=1-\frac{q_4}{h}\omega,
\tag{B.4}
$$

$$
\begin{aligned}
p_1 &= \frac{\partial P_{11}}{\partial t}=\mathrm{e}^{-\zeta t_1}[\zeta(A_1(\zeta\cos(\omega_{d1}t_1)+\omega_{d1}\sin(\omega_{d1}t_1))\\
&\quad +A_2(\zeta\sin(\omega_{d1}t_1)-\omega_{d1}\cos(\omega_{d1}t_1)))+A_1\big(\zeta\omega_{d1}\sin(\omega_{d1}t_1)-\omega_{d1}^2\cos(\omega_{d1}t_1)\big)\\
&\quad +A_2(-\zeta\omega_{d1}\cos(\omega_{d1}t_1)-\omega_{d1}^2\sin(\omega_{d1}t_1))\big]\\
&\quad -B_1\omega^2\sin(\omega t_1+\tau_0)-B_2\omega^2\cos(\omega t_1+\tau_0),\\
p_2 &= \frac{\partial P_{11}}{\partial t}=\mathrm{e}^{-\eta t_1}(-\eta(A_3\cos(\omega_{d2}t_1)+A_4\sin(\omega_{d2}t_1))\\
&\quad +\omega_{d2}(-A_3\sin(\omega_{d2}t_1)+A_4\cos(\omega_{d2}t_1)))+B_3\omega\cos(\omega t_1+\tau_0)-B_4\omega\sin(\omega t_1+\tau_0),\\
p_3 &= \frac{\partial P_{13}}{\partial t}=\mathrm{e}^{-\eta t_1}[\eta(A_3(\eta\cos(\omega_{d2}t_1)+\omega_{d2}\sin(\omega_{d2}t_1))\\
&\quad +A_4(\eta\sin(\omega_{d2}t_1)-\omega_{d2}\cos(\omega_{d2}t_1)))+A_3\big(\eta\omega_{d2}\sin(\omega_{d2}t_1)-\omega_{d2}^2\cos(\omega_{d2}t_1)\big)\\
&\quad +A_4(-\eta\omega_{d2}\cos(\omega_{d2}t_1)-\omega_{d2}^2\sin(\omega_{d2}t_1))\big]-B_3\omega^2\sin(\omega t_1+\tau_0)-B_4\omega^2\cos(\omega t_1+\tau_0),
\end{aligned}
\tag{B.5}
$$

$$
\begin{aligned}
q_1 &= \frac{\partial G}{\partial\dot{x}_{10}}=-\frac{1}{\omega_{d1}}\mathrm{e}^{-\zeta t_1}\sin(\omega_{d1}t_1),\\
q_2 &= \frac{\partial G}{\partial x_{20}}=\mathrm{e}^{-\eta t_1}\left(\cos(\omega_{d2}t_1)+\frac{\eta}{\omega_{d2}}\sin(\omega_{d2}t_1)\right)-\mathrm{e}^{-\zeta t_1}\left(\cos(\omega_{d1}t_1)+\frac{\zeta}{\omega_{d1}}\sin(\omega_{d1}t_1)\right),\\
q_3 &= \frac{\partial G}{\partial\dot{x}_{20}}=\frac{1}{\omega_{d2}}\mathrm{e}^{-\eta t_1}\sin(\omega_{d2}t_1),
\end{aligned}
$$

$$q_4 = \frac{\partial G}{\partial \tau_0} = \mathrm{e}^{-\eta t_1}\Bigg((-B_3c_0 + B_4s_0)\cos(\omega_{d2}t_1) + \frac{1}{\omega_{d2}}((-\eta B_3 + \omega B_4)c_0 + (\eta B_4 + \omega B_3)s_0)\sin(\omega_{d2}t_1)\Bigg), \tag{B.6}$$

$$\begin{aligned} h = \frac{\partial G}{\partial t} = {} & \mathrm{e}^{-\eta t_1}[-\eta(A_3\cos(\omega_{d2}t_1) + A_4\sin(\omega_{d2}t_1)) \\ & + \omega_{d2}(-A_3\sin(\omega_{d2}t_1) + A_4\cos(\omega_{d2}t_1))] + \mathrm{e}^{-\zeta t_1}[\zeta(A_1\cos(\omega_{d1}t_1) + A_2\sin(\omega_{d1}t_1)) \\ & - \omega_{d1}(-A_1\sin(\omega_{d1}t_1) + A_2\cos(\omega_{d1}t_1))] + (B_3\omega - B_1\omega)\cos(\omega t_1 + \tau_0) \\ & + (B_2\omega - B_4\omega)\sin(\omega t_1 + \tau_0). \end{aligned} \tag{B.7}$$

Appendix C

The eigenvalues of the Jacobian matrix: $u_m = 1.5$, $u_c = 1$, $u_k = 1$, $\zeta = 0.0001$, $f_2 = 0.2$, $R = 0.8$, $\omega = 2.2$ (b_f is taken as a control parameter).

b_f	0.155	0.18	0.194618	0.2	0.2570	0.285
λ_1	2.7226	1.6250	1.0000	$0.6283+0.1266i$	$0.0304+0.6390i$	$-0.1570+0.6183i$
λ_2	0.1590	0.2529	0.4180	$0.6283-0.1266i$	$0.0304-0.6390i$	$-0.1570-0.6183i$
λ_3	$-0.8310+0.5525i$	$-0.8302+0.5538i$	$-0.8278+0.5611i$	$-0.8295+0.5551i$	$-0.8278+0.5611i$	$-0.8279+0.5659i$
λ_4	$-0.8310-0.5525i$	$-0.8302-0.5538i$	$-0.8278-0.5611i$	$-0.8295-0.5551i$	$-0.8278-0.5611i$	$-0.8295-0.5659i$
$\lvert\lambda_1\rvert$	2.7266	1.6250	1.0000	0.6409	0.6390	0.6379
$\lvert\lambda_2\rvert$	0.1509	0.2529	0.4108	0.6409	0.6390	0.6379
$\lvert\lambda_3\rvert$	0.9979	0.9979	0.9980	0.9981	1.0000	1.0028
$\lvert\lambda_4\rvert$	0.9979	0.9979	0.9980	0.9981	1.0000	1.0028

Appendix D

The eigenvalues of the Jacobian matrix: $u_m = 1$, $u_c = 1$, $u_k = 2$, $\zeta = 0.0001$, $f_2 = 0.2$, $R = 0.8$, $b_f = 0.08$ (ω is taken as a control parameter).

ω	1.6500	1.65820	1.8000	3.00207	3.1000	3.4205	3.5000
λ_1	$0.6236+0.1845i$	1.0000	3.0402	1.0000	$0.5603+0.3143i$	$0.1438+0.6234i$	$0.0564+0.6356i$
λ_2	$0.6236-0.1845i$	0.4203	0.1385	0.4133	$0.5603-0.3143i$	$0.1438-0.6234i$	$0.0564-0.6356i$
λ_3	$-0.0862+0.9795i$	$-0.1041+0.9779i$	$-0.4202+0.8917i$	$-0.8299+0.5489i$	$-0.7823+0.6158i$	$-0.6164+0.7874i$	$-0.5749+0.8213i$
λ_4	$-0.0862-0.9795i$	$-0.1041-0.9779i$	$-0.4202-0.8917i$	$-0.8209-0.5489i$	$-0.7823-0.6158i$	$-0.6164-0.7874i$	$-0.5749-0.8213i$
$\lvert\lambda_1\rvert$	0.6540	1.0000	3.0402	1.0000	0.6425	0.6398	0.6381
$\lvert\lambda_2\rvert$	0.6540	0.4203	0.1385	0.4132	0.6425	0.6398	0.6381
$\lvert\lambda_3\rvert$	0.9833	0.9834	0.9858	0.9951	0.9957	1.0000	1.0026
$\lvert\lambda_4\rvert$	0.9833	0.9834	0.9858	0.9951	0.9957	1.0000	1.0026

References

[1] S.W. Shaw, P.J. Holmes, A periodically forced piecewise linear oscillator, *Journal of Sound and Vibration* 90 (1983) 129–155.
[2] A.B. Nordmark, Non-periodic motion caused by grazing incidence in an impact oscillator, *Journal of Sound and Vibration* 145 (1991) 279–297.
[3] C. Budd, F. Dux, A. Cliffe, The effect of frequency and clearance variations on single-degree-of-freedom impact oscillators, *Journal of Sound and Vibration* 184 (1995) 475–502.
[4] L.N. Virgin, C.J. Begley, Grazing bifurcations and basins of attraction in an impact-friction oscillator, *Physica D* 130 (1999) 43–57.
[5] S.L.T. de Souza, I.L. Caldas, Calculation of Lyapunov exponents in systems with impacts, *Chaos, Solitons and Fractals* 19 (2004) 569–579.

[6] G.W. Luo, J.H. Xie, Stability of periodic motion, bifurcations and chaos of a two-degree-of-freedom vibratory system with symmetrical rigid stops, *Journal of Sound and Vibration* 273 (2004) 543–568.
[7] W.C. Ding, J.H. Xie, Q.G. Sun, Interaction of Hopf and period doubling bifurcations of a vibro-impact system, *Journal of Sound and Vibration* 275 (2004) 27–45.
[8] J.H. Xie, W.C. Ding, Hopf–Hopf bifurcation and invariant torus $\mathbf{T}^2$ of a vibro-impact system, *International Journal of Non-Linear Mechanics* 40 (2005) 531–543.
[9] D.J. Wagg, Rising phenomena and the multi-sliding bifurcation in a two-degree-of-freedom impact oscillator, *Chaos, Solitons and Fractals* 22 (2004) 541–548.
[10] A. Ben-Tal, Symmetry restoration in a class of forced oscillators, *Physica D* 171 (2002) 236–248.
[11] K. Yu, A.C.J. Luo, The periodic impact responses and stability of a human body in a vehicle traveling on rough terrain, *Journal of Sound and Vibration* 272 (2004) 267–286.
[12] A.C.J. Luo, L. Chen, Periodic motions and grazing in a harmonically forced, piecewise, linear oscillator with impacts, *Chaos, Solitons and Fractals* 24 (2005) 567–578.